

nature

The Living Record of Science 《自然》百年科学经典

(英汉对照版)

第八卷

总顾问：李政道 (Tsung-Dao Lee)

英方主编：Sir John Maddox 中方主编：路甬祥
 Sir Philip Campbell

VIII 1993-1997

VI 1975-1992

IV 1949-1974

II 1921-1948

IX 1998-2000

VII 1993-1997

V 1975-1992

III 1924-1948

I 1998-1997

外语教学与研究出版社 · 麦克米伦教育 · 自然科研

FOREIGN LANGUAGE TEACHING AND RESEARCH PRESS · MACMILLAN EDUCATION · NATURE RESEARCH

nature

The Living Record of Science

《自然》百年科学经典



(英汉对照版)

第八卷

总顾问：李政道 (Tsung-Dao Lee)

英方主编：Sir John Maddox 中方主编：路甬祥
 Sir Philip Campbell

(VIII)

1993-1997



外语教学与研究出版社 · 麦克米伦教育 · 自然科研

FOREIGN LANGUAGE TEACHING AND RESEARCH PRESS · MACMILLAN EDUCATION · NATURE RESEARCH

北京 BEIJING

Original English Text © Macmillan Publishers Limited
Chinese Translation © Foreign Language Teaching and Research Press

This edition is published under arrangement with Macmillan Publishers (China) Limited. It is for sale in the People's Republic of China only, excluding Hong Kong SAR, Macao SAR and Taiwan Province, and may not be bought for export therefrom.

图书在版编目 (CIP) 数据

《自然》百年科学经典. 第八卷, 1993 ~ 1997; 英汉对照 / (英) 约翰·马多克斯 (John Maddox), (英) 菲利普·坎贝尔 (Philip Campbell), 路甬祥主编. — 北京: 外语教学与研究出版社, 2017.2

ISBN 978-7-5135-8560-6

I. ①自… II. ①约… ②菲… ③路… III. ①自然科学—文集—英、汉 IV. ①N53

中国版本图书馆 CIP 数据核字 (2017) 第 036827 号

出版人 蔡剑峰
项目统筹 章思英 Charlotte Liu (加拿大)
项目负责 刘晓楠 黄小斌 Chris Balderston (美)
责任编辑 黄小斌
执行编辑 张梦璇 王丽霞
封面设计 孙莉明 平原
出版发行 外语教学与研究出版社
社址 北京市西三环北路 19 号 (100089)
网址 <http://www.fltrp.com>
印刷 北京华联印刷有限公司
开本 787 × 1092 1/16
印张 71
版次 2017 年 6 月第 1 版 2017 年 6 月第 1 次印刷
书号 ISBN 978-7-5135-8560-6
定价 568.00 元

购书咨询: (010) 88819926 电子邮箱: club@fltrp.com
外研书店: <https://waiyants.tmall.com>
凡印刷、装订质量问题, 请联系我社印制部
联系电话: (010) 61207896 电子邮箱: zhijian@fltrp.com
凡侵权、盗版书籍线索, 请联系我社法律事务部
举报电话: (010) 88817519 电子邮箱: banquan@fltrp.com
法律顾问: 立方律师事务所 刘旭东律师
中咨律师事务所 殷斌律师
物料号: 285600001

《自然》百年科学经典（英汉对照版）

总顾问：李政道（Tsung-Dao Lee）

英方主编：Sir John Maddox 中方主编：路甬祥

Sir Philip Campbell

编审委员会

英方编委：

Philip Ball

Vikram Savkar

David Swinbanks

中方编委（以姓氏笔画为序）：

许智宏

赵忠贤

滕吉文

本卷审稿专家（以姓氏笔画为序）

王二七	王社江	毛淑德	文 波	方向东	石 磊	田立德
刘冬生	齐利民	许家喜	孙 松	杜 忆	杜爱民	李 彦
李 娟	李军刚	李忠海	李铁刚	杨崇林	吴 晶	吴学兵
吴新智	何香涛	张华伟	张颖奇	陆朝阳	陈 文	欧阳自远
周礼勇	周济林	赵凌霞	胡松年	胡卓伟	段克勤	秦志海
徐永福	郭建栋	黄宝春	常 燎	崔娅铭	梁晓峰	韩汝珊
焦炳华	臧伟呈	翟天瑞	黎 卓			

编译委员会

本卷翻译工作组稿人 (以姓氏笔画为序)

王帅帅	王晓蕾	王耀杨	刘 明	刘晓楠	关秀清	李 琦
何 铭	沈乃澂	张 健	陈 林	郭红锋	黄小斌	蔡 迪

本卷翻译人员 (以姓氏笔画为序)

王振华	王耀杨	元旭津	毛晨晖	冯 翀	刘 霞	刘皓芳
齐红艳	苏怡汀	李 梅	李 琦	李海宁	肖 莉	何 钧
沈乃澂	张锦彬	陈 林	武振宇	金 煜	金世超	周 杰
周志华	俞贵平	莫维克	钱 磊	高俊义	葛聆飒	

本卷校对人员 (以姓氏笔画为序)

马 昊	王振华	卢 皓	邢 波	邢路达	吉 祥	朱晓霞
任进成	刘汾汾	刘雨佳	刘项琨	刘萍萍	许静静	严宏强
李 乐	李 婷	李梦桃	李霄霞	杨 晶	邱珍琳	邱彩玉
何 敏	何映晖	汪 涵	张 狄	张 焕	张 晴	陈贝贝
欧阳叶昀	周小雅	郑旭峰	宗伟凯	房秋怡	荣金诚	贺乐天
钱 磊	郭 谱	郭晓博	龚文瑜	葛聆飒	董静娟	韩涛涛
Elizabeth Ng (加拿大)		Eric Leher (澳)				

Contents

目录

The “Flickering Switch” of Late Pleistocene Climate Change	2
晚更新世气候变化的“闪电变换”	3
Recent Change of Arctic Tundra Ecosystems from a Net Carbon Dioxide Sink to a Source	16
近期北极冻原生态系统的净二氧化碳汇到源的转变	17
Effects of an Endothermic Phase Transition at 670 km Depth in a Spherical Model of Convection in the Earth’s Mantle	30
地球内部 670 km 深度处的矿物吸热相变对地幔对流模式的影响	31
SNAP Receptors Implicated in Vesicle Targeting and Fusion	54
囊泡靶向及融合过程中 SNAP 受体的功能	55
Discovery of the Candidate Kuiper Belt Object 1992 QB ₁	82
柯伊伯带天体候选体 1992 QB ₁ 的发现	83
Superconductivity above 130 K in the Hg–Ba–Ca–Cu–O System	94
Hg–Ba–Ca–Cu–O 体系在 130 K 以上时的超导性	95
Single-shell Carbon Nanotubes of 1-nm Diameter	104
直径 1 nm 的单层碳纳米管	105
Cobalt-catalysed Growth of Carbon Nanotubes with Single-atomic-layer Walls	114
具有单原子层管壁的碳纳米管的钴催化生长	115
The Displacement Field of the Landers Earthquake Mapped by Radar Interferometry	124
雷达干涉测量技术得到的兰德斯地震位移场	125
Climate Instability during the Last Interglacial Period Recorded in the GRIP Ice Core	140
GRIP 冰芯记录的末次间冰期气候的不稳定性	141
Evidence for General Instability of Past Climate from a 250-kyr Ice-core Record	162
冰芯记录的过去 25 万年来总体气候不稳定性的证据	163

Extending the Vostok Ice-core Record of Palaeoclimate to the Penultimate Glacial Period	176
把沃斯托克冰芯的古气候记录延伸至倒数第二次冰期.....	177
B-cell Apoptosis Induced by Antigen Receptor Crosslinking is Blocked by a T-cell Signal Through CD40.....	202
T细胞通过CD40抑制抗原受体交联引起的B细胞凋亡.....	203
Correlations between Climate Records from North Atlantic Sediments and Greenland Ice.....	218
北大西洋沉积物与格陵兰冰芯气候记录之间的相关性.....	219
Music and Spatial Task Performance.....	236
音乐和空间任务表现.....	237
Possible Gravitational Microlensing of a Star in the Large Magellanic Cloud.....	240
大麦哲伦云的一颗恒星可能存在微引力透镜效应.....	241
Evidence for Gravitational Microlensing by Dark Objects in the Galactic Halo.....	252
利用微引力透镜效应发现银晕中存在暗天体的证据.....	253
A Search for Life on Earth from the Galileo Spacecraft.....	266
用伽利略木星探测器探测地球生命.....	267
Total Synthesis of Taxol	294
紫杉醇的全合成.....	295
A Cell Initiating Human Acute Myeloid Leukaemia after Transplantation into SCID Mice	312
一种植入SCID小鼠中引发人急性髓性白血病的细胞.....	313
2.2 Mb of Contiguous Nucleotide Sequence from Chromosome III of <i>C. elegans</i>	328
秀丽隐杆线虫3号染色体上的2.2 Mb连续核苷酸序列.....	329
The First Skull and Other New Discoveries of <i>Australopithecus afarensis</i> at Hadar, Ethiopia	358
在埃塞俄比亚的哈达尔发现的第一例南方古猿阿法种的头骨和其他新发现.....	359
Deuterium Abundance and Background Radiation Temperature in High-redshift Primordial Clouds.....	372
高红移原初气体云中的氘丰度和背景辐射温度.....	373

A Diverse New Primate Fauna from Middle Eocene Fissure-fillings in Southeastern China	396
中国东南部中新世裂隙堆积中新发现的一个多样化灵长类动物群	397
Chemical Self-replication of Palindromic Duplex DNA	422
回文双链DNA的化学自我复制	423
Self-replication of Complementary Nucleotide-based Oligomers	436
互补配对的寡聚核苷酸的自我复制	437
Testing the Iron Hypothesis in Ecosystems of the Equatorial Pacific Ocean	452
在赤道太平洋海域生态系统中对铁假说的验证	453
Iron Limitation of Phytoplankton Photosynthesis in the Equatorial Pacific Ocean ...	480
赤道太平洋海域铁对浮游植物光合作用的限制	481
<i>Australopithecus ramidus</i> , a New Species of Early Hominid from Aramis, Ethiopia	494
在埃塞俄比亚的阿拉米斯发现的一种新型的早期原始人类物种 ——南方古猿始祖种	495
Evidence from Gravity and Topography Data for Folding of Tibet	524
青藏高原的褶皱作用：来自重力和地形资料的证据	525
DNA Fingerprinting Dispute Laid to Rest	548
DNA 指纹分析争议的平息	549
Distance to the Virgo Cluster Galaxy M100 from Hubble Space Telescope Observations of Cepheids	570
由哈勃空间望远镜观测造父变星到室女星系团成员星系 M100 的距离	571
Massive Iceberg Discharges as Triggers for Global Climate Change	592
大规模冰筏涌出是全球气候变化的触发器	593
Positional Cloning of the Mouse <i>obese</i> Gene and Its Human Homologue	612
小鼠肥胖基因及其人类同源基因的定位克隆	613
Viral Dynamics in Human Immunodeficiency Virus Type 1 Infection	640
人免疫缺陷病毒 1 型感染的病毒动力学研究	641
Rapid Turnover of Plasma Virions and CD4 Lymphocytes in HIV-1 Infection	668
HIV-1 感染患者血浆内病毒粒子和 CD4 淋巴细胞的快速更新	669

A Plio-Pleistocene Hominid from Dmanisi, East Georgia, Caucasus	684
在高加索格鲁吉亚东部的德马尼西发现的上新世 – 更新世时期的原始人类	685
Gravitationally Redshifted Emission Implying an Accretion Disk and Massive Black Hole in the Active Galaxy MCG-6-30-15	700
活动星系 MCG-6-30-15 的引力红移辐射暗示吸积盘和大质量黑洞的存在	701
A Three-dimensional Self-consistent Computer Simulation of a Geomagnetic Field Reversal	712
地磁场倒转的三维自洽计算机模拟	713
Bifurcations of the Atlantic Thermohaline Circulation in Response to Changes in the Hydrological Cycle	736
大西洋热盐环流的分岔对水文循环的响应	737
A Jupiter-mass Companion to a Solar-type Star	762
类太阳恒星的一个类木伴星	763
Sequence Variation of the Human Y Chromosome	782
人类 Y 染色体的序列变异	783
Asymmetric Autocatalysis and Amplification of Enantiomeric Excess of a Chiral Molecule	792
不对称自催化与手性分子对映体过量值的放大	793
Sheep Cloned by Nuclear Transfer from a Cultured Cell Line	802
从体外培养的细胞系中通过核移植获得克隆羊的方法	803
A Comprehensive Genetic Map of the Mouse Genome	814
一张高精度的小鼠基因组遗传图谱	815
Orbital Migration of the Planetary Companion of 51 Pegasi to Its Present Location ...	832
飞马座 51 的行星型伴星轨道迁移到现在位置的过程	833
A 3.5-Gyr-old Galaxy at Redshift 1.55	842
红移 1.55 处的一个年龄为 3.5 Gyr 的星系	843
A Search for Human Influences on the Thermal Structure of the Atmosphere	860
人类对大气温度结构影响的研究	861
Seismological Evidence for Differential Rotation of the Earth's Inner Core	892
地球内核差异性旋转的地震学证据	893

A DNA-based Method for Rationally Assembling Nanoparticles into Macroscopic Materials	914
一种基于 DNA 将纳米颗粒合理组装成宏观材料的方法	915
Organization of “Nanocrystal Molecules” Using DNA	928
利用 DNA 来实现“纳米晶体分子”的组装	929
Discovery of Ganymede’s Magnetic Field by the Galileo Spacecraft	940
伽利略木星探测器发现木卫三的磁场	941
Gravitational Scattering as a Possible Origin for Giant Planets at Small Stellar Distances	956
引力散射是近邻巨行星的可能起源	957
2.5-million-year-old Stone Tools from Gona, Ethiopia	968
埃塞俄比亚戈纳发现 250 万年前石制工具	969
Viable Offspring Derived from Fetal and Adult Mammalian Cells	988
胎儿和成年哺乳动物的细胞可以产生存活后代	989
Evidence for Deep Mantle Circulation from Global Tomography	1002
深部地幔流动的 global 层析成像证据	1003
Transient Optical Emission from the Error Box of the γ-ray Burst of 28 February 1997	1028
1997 年 2 月 28 日伽马射线暴误差框内的暂现光学辐射	1029
Spectral Constraints on the Redshift of the Optical Counterpart to the γ-ray Burst of 8 May 1997	1044
对 1997 年 5 月 8 日伽马射线暴光学对应体红移的光谱限制	1045
Size and Morphology of the Chicxulub Impact Crater	1056
希克苏鲁伯撞击坑的大小和形态	1057
Experimental Quantum Teleportation	1080
量子隐形传态实验	1081
Localization of Light in a Disordered Medium	1104
无序介质中光的局域化	1105
Appendix: Index by Subject	
附录: 学科分类目录	1121

Volume VIII
(1993-1997)

The “Flickering Switch” of Late Pleistocene Climate Change

K. C. Taylor *et al.*

Editor’s Note

This paper astonished the palaeoclimate community by revealing that significant shifts in climate can occur extremely rapidly, perhaps on timescales of just 5–20 years. Kendrick Taylor and colleagues used measurements of the electrical conductivity of an ice core drilled at Greenland to obtain a record of changes in the dust content of the ice during the last ice age. Alkaline dust alters the conductivity, and changes in airborne dust content reflect climate-induced rearrangements of atmospheric circulation. The researchers found several bursts of sudden changes, which they attribute to abrupt switches between two different climate states. These results suggest that climate change might not be a gradual affair, but could be triggered suddenly when critical thresholds are surpassed.

Polar ice contains a unique record of past climate variations; previous Greenland ice cores have documented relatively warm “interstadial” periods during the last glaciation and short (century-scale) returns to colder conditions during the glacial to interglacial warming (see, for example, ref. 1). These climate features have also been observed to varying degrees in ocean sediment cores²⁻⁴ and terrestrial pollen and insect records⁵⁻⁷. Here we report electrical conductivity measurements from a new Greenland ice core, which confirm these previous observations, and also reveal a hitherto unrecognized mode of rapid climate variation. Fluctuations in ice conductivity on the scales of < 5–20 years reflect rapid oscillations in the dust content of the atmosphere. This “flickering” between two preferred states would seem to require extremely rapid reorganizations in atmospheric circulation.

THE Greenland Ice-Sheet Project 2 (GISP2) is coring the summit of the Greenland ice sheet (72.6° N, 38.5° W) to develop a continuous high-resolution record of climate related parameters going back at least 200,000 years. The electrical conductivity measurement (ECM) measures the ability of an ice core to conduct an electrical current, which is related to the balance of acids and bases in the ice⁸⁻¹⁰. The measurement is made by determining the current flowing between two moving electrodes with a potential difference of a few thousand volts. The current increases with increased concentration of strong acids, especially sulphuric (from volcanic activity⁸ and other sources¹¹) and nitric (controlled mainly by atmospheric chemistry^{12,13}). The current decreases when the acids are neutralized, which is most commonly caused by ammonia (biomass burning and other sources^{14,15}) or due to alkaline dust (continental sources¹²).

晚更新世气候变化的“闪电变换”

泰勒等

编者按

本文通过揭示气候可能仅在5~20年间就会发生极速变化而使古气候研究学者们感到惊讶。肯德里克·泰勒和同事们测量了在格陵兰钻到的冰芯的电导率，以获取在末次冰期期间冰芯中粉尘含量的变化记录。碱性粉尘改变了电导率，而空气中携带的粉尘含量的变化能够反映大气环流引起的气候变迁。研究人员发现气候发生了数次突然变化，并将其归因为两种不同气候条件之间的突然转换。这些结果表明，气候变化可能不是渐变发生的，而有可能是超过临界值时被突然引发的。

极地冰芯中包含着独特的古气候变化记录；先前对格陵兰冰芯的研究已经证明：末次冰期时存在相对较温暖的“间冰阶”，并且由冰期向间冰期过渡的总变暖趋势下也曾出现过短暂（百年尺度）的回冷气候（参见文献1）。海洋沉积物岩芯^[2-4]及大陆孢粉与昆虫记录^[5-7]中也不同程度地观测到了上述气候特征。本文将介绍一个格陵兰冰芯电导率的新的测定结果，该测定结果不仅证实了上述观测结果，而且揭示出了一个迄今还未识别出的快速气候变化模式。<5~20年尺度上的冰芯电导率的波动反映了大气中粉尘含量的快速振荡。两个主要阶段之间出现的这种“闪电式变化”似乎是大气环流极速重组的结果。

格陵兰冰盖计划2 (GISP2)的目的是钻取格陵兰冰盖顶部萨米特冰芯(72.6° N, 38.5° W)以获取至少20万年以来的连续高分辨率气候记录的相关参数。电导率测量法(ECM)测量的是冰芯传导电流的能力，与冰芯中酸性与碱性的平衡有关^[8-10]。该测量方法是通过确定势差数千伏的两个运动电极之间流过的电流来进行的。电流随强酸，特别是硫酸(来自火山活动^[8]和其他来源^[11])和硝酸(主要受大气化学作用的控制^[12,13])浓度的增加而增大。当酸性物质被中和时，电流将减小，这种中和作用通常是由氨气(生物体的燃烧以及其他来源^[14,15])或碱性粉尘(来源于大陆^[12])所致。

Changes in the value of the ECM baseline occur when climate or weather patterns change the source strength or transport of the acids and bases. During Wisconsinian times, dust transport to Greenland increased by at least a factor of 40, possibly because of changes in transport paths, wind speeds and surface moisture¹⁶. The large amounts of alkaline dust present in ice from cold periods during the last glacial period neutralize the acids, reducing the current flow between the electrodes by a factor of ~ 40 compared with Holocene conditions. This permits clear discrimination between dusty and less dusty conditions. The relationship between the ECM signal and the concentration of alkaline dust at the transition from acidic to alkaline conditions (0 to 10 μA) is not well quantified. At the transition between acidic and alkaline conditions, the effect of small amounts of additional dust on the magnitude (but not the frequency) of the ECM signal may be disproportionately large. In the GISP2 core, however, detailed chemical analysis shows that the order-of-magnitude decreases in ECM that we consider here are associated with order-of-magnitude increases in calcium. The source for the calcium is believed to be airborne calcium carbonate dust. The ECM record has the highest time resolution (> 15 samples per year) of available measurements, and together with the sensitivity to dust, this makes ECM suitable for investigating the rate of rapid atmospheric circulation changes.

The ECM record discussed here covers the time period 10 to 42 thousand years before present (kyr BP), and allows climate variability to be investigated on timescales of seasons to millennia (Fig. 1a). The core has been preliminarily dated by counting of annual layers which are identified by visual stratigraphy, ECM and particulate measurements. Every annual layer has been counted for the past 17.4 kyr BP with an estimated accuracy of 3% (ref. 17). Between 17.4 and 40.5 kyr BP, annual layers were counted by visual stratigraphy for one out of every 10 or 20 m. The interim sections were dated by counting interpolated annual layers. At an age of 15 kyr BP, ages of identical events in the GISP2 core and GRIP core¹ (located 30 km to the east) differ by 200 years. This is within expected errors. At an age of 40 kyr BP in the GISP2 core, corresponding events in the GRIP core are dated at 34 kyr BP. Both groups are refining the preliminary dating of the cores and this discrepancy is likely to diminish. A comparison of the two cores will be presented elsewhere.

当气候或天气类型导致酸性或碱性物质的来源或搬运方式发生改变时，ECM 基线值就会出现相应变化。威斯康星冰期时，粉尘向格陵兰岛的输送至少增加了 39 倍，可能是由输送路径、风速以及海表湿度的改变所致^[16]。在末次冰期的冷期冰芯中，大量碱性粉尘的出现使酸性物质被中和，使得电极间的电流减少为全新世的 1/40。据此可清楚地辨别出多粉尘和无粉尘环境条件。在酸碱性之间的过渡环境中 (0~10 μA)，ECM 信号与碱性粉尘浓度之间的关系还未得到很好的量化。因为在酸碱性之间的过渡环境中，少量额外粉尘即可能对 ECM 信号的大小 (不会影响频率) 产生巨大影响。不过，利用 GISP2 冰芯进行详细的化学分析表明，本文我们所关注的 ECM 信号的衰减量级与钙元素的增加量级有关。而降落的碳酸盐粉尘被认为是这些钙的主要来源。由于 ECM 记录具有所有可测量方法中最高的时间分辨率 (> 15 个样品每年)，并且对粉尘具有较强的敏感性，这使得 ECM 非常适合于大气循环快速变化的研究。

本文所讨论的 ECM 记录跨越了距今 1 万年前到 4.2 万年前的时段，可以据此研究季节性尺度到千年尺度上的气候变化 (图 1a)。通过对可视地层学、ECM 和粒子测量分辨出的年层进行计数，学者对冰芯作了初步的定年。从中确定了过去 1.74 万年以来所有的年层年代，年代误差约为 3% (参见文献 17)。从距今 1.74 万年前到 4.05 万年前的年层年代是利用可视地层学方法数出的，这样的地层大约每 10~20 m 一个。中间的部分则是通过内插法确定的。在距今 1.5 万年前，GISP2 冰芯和 GRIP 冰芯^[1] (GRIP 位于 GISP2 以东约 30 km 处) 中相同事件的年龄相差 200 年。该值位于预期的误差范围以内。在 GISP2 冰芯中测年结果为 4 万年的事件对应于 GRIP 冰芯中的测年结果为 3.4 万年。两组数据都对冰芯的初步测年结果作了改进以尽可能减小这个差异。两冰芯的对比结果将另文给出。

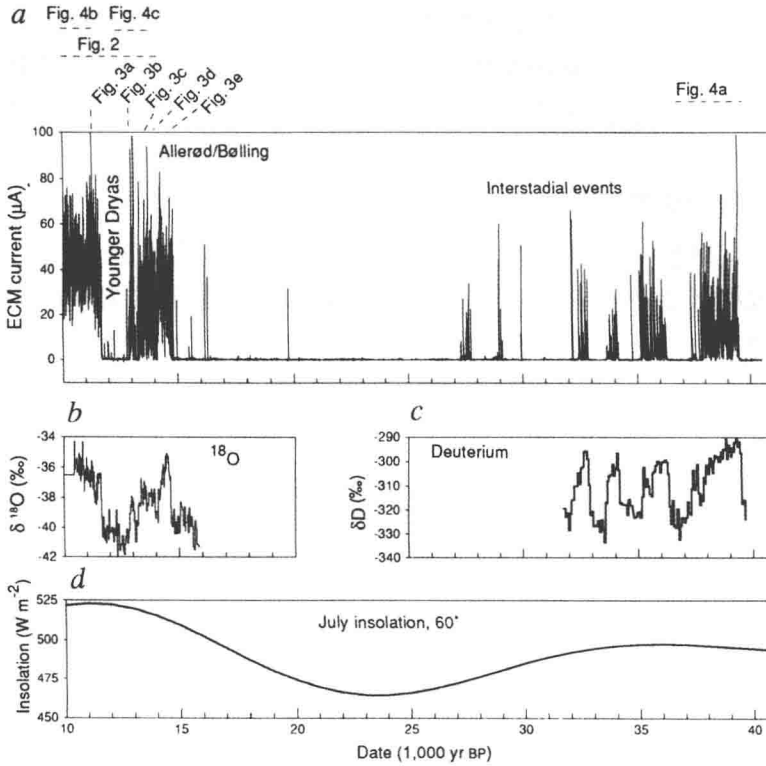


Fig. 1. *a*, GISP2 electrical conductivity measurement (ECM) record for the period of 10–40.5 kyr BP. Low current levels indicate that alkaline dust has neutralized the acidity of the ice. The record is resampled to a rate of one sample per year. The ages of the other expanded-scale figures (Figs 2–4) are indicated. The years indicated are calendar years. We adopt the carbon-14 datum of AD 1950 as present time. *b*, Isotopic ratio $^{18}\text{O}/^{16}\text{O}$ for the ages 10.5 to 16 kyr BP. *c*, Isotopic ratio D/H for the ages 32 to 40.5 kyr BP. The isotope samples are from contiguous 1-m sections of the core. Because of flow-induced thinning of annual layers, the 1-m sections correspond to one sample every 15 to 37 years in the $^{18}\text{O}/^{16}\text{O}$ record and one sample every 65 to 80 years in the deuterium/hydrogen record. The correlation between the ECM and the isotope records demonstrates that the ECM record is responding to climatic events. *d*, Mean July insolation for latitude 60° north²³.

The ECM record is characterized by a bimodal high or low pattern that is controlled by the absence or presence of alkaline dust. For comparison we also present stable isotope profiles, which are known to respond to the temperature difference between the moisture source and the ice deposition site, and are used extensively for palaeoclimate reconstructions^{18–20}. The synchronous transitions in the ECM and isotope records (Fig. 1*b*, *c*) demonstrate the sensitivity of the ECM to climate conditions. Periods of heavy isotopic composition indicate warmer interglacial or interstadial conditions. The high ECM values during these times indicate that it was also less dusty. The ECM record (Fig. 2) clearly shows well-known millennium-scale Younger Dryas, Allerød, Bølling and Interstadial periods, and century-scale events during the Allerød and Bølling periods. The isolated spikes on the ECM record span at most a few years and are likely to be associated with volcanic activity. Although isotopes and ECM show synchronous transitions in Fig. 1, they do not correlate well on timescales of a few years. This indicates that they respond to different aspects of

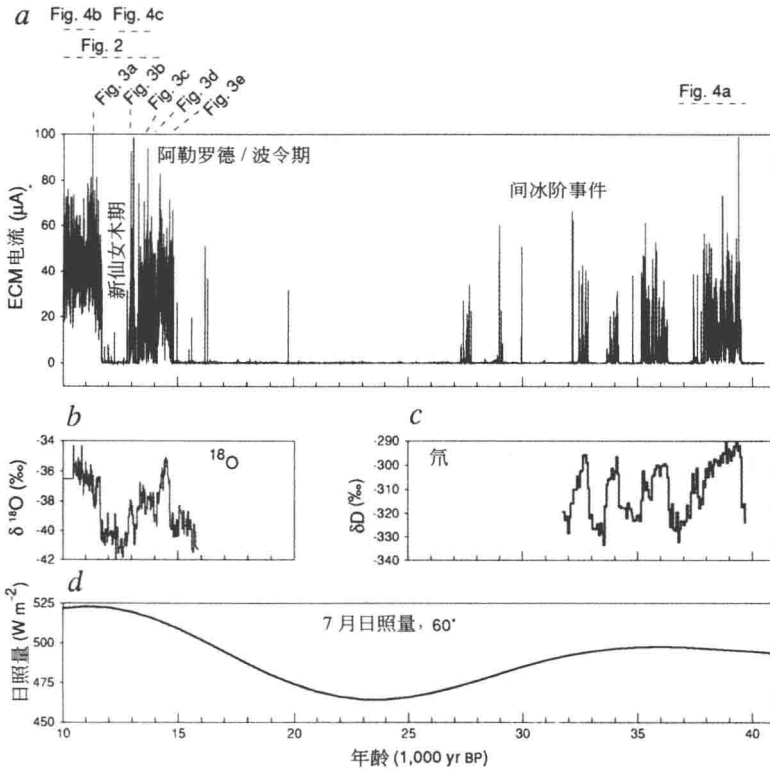


图 1. *a*, 距今 1 万年前至 4.05 万年前间, GISP2 电导率测量结果 (ECM) 记录曲线。电流较低时表示碱性粉尘中和了冰川中的酸性物质。该记录的重复取样率为每年一个样品。图中还给出了局部放大图 (图 2~4) 的年龄, 所标的年龄为历年。其中以 ^{14}C 测年得到的公元 1950 年为当前时间。*b*, 距今 1.05 万年前至 1.6 万年前间, 氧同位素比值 $^{18}\text{O}/^{16}\text{O}$ 的变化曲线。*c*, 距今 3.2 万年前至 4.05 万年前间, 氢同位素比值 D/H 的变化曲线。同位素样品均来自冰芯中连续长为 1 m 的一段。由于水流引起的年层减薄效应, 1 m 间隔相当于 $^{18}\text{O}/^{16}\text{O}$ 记录中每 15~37 年一个样品, 在 D/H 记录中相当于每 65~80 年一个样品。ECM 与同位素之间的相关性证明, ECM 记录与气候事件是对应的。*d*, 北纬 60° 上 7 月份的平均太阳辐射^[23]。

ECM 记录以双峰或双谷为特征, 受碱性粉尘存在与否的影响。此外我们还给出了稳定同位素变化曲线, 以便于对比。大家都知道该曲线是与水分来源地和冰芯沉积地点之间的温度差异相对应的, 并且已在古气候重建中得到广泛应用^[18-20]。ECM 和同位素记录的同步变化 (图 1*b* 和 *c*) 证明了 ECM 对气候条件变化的敏感性。重同位素组分阶段代表较温暖的间冰期或间冰阶环境。这些时段上出现的高 ECM 值说明当时大气中的粉尘含量较少。ECM 记录 (图 2) 清楚地显示出了众所周知的千年尺度上的新仙女木期、阿勒罗德期、波令期和间冰阶以及阿勒罗德期和波令期之间百年尺度的气候事件。ECM 记录上的孤立尖峰跨越的时间最大仅为数年, 很可能与火山活动有关。虽然从图 1 来看, 同位素和 ECM 表现为同步变化, 但在数年的时间尺度上两者的相关性并不好。这说明它们反映了气候变化的不同方面 (温度和粉尘),